J. Membrane Biol. 155, 143–156 (1997)

The Journal of
Membrane
Biology

Permeation Properties of Na^+ and Ca^{2+} Ions through the Mouse ϵ_2/ζ_1 NMDA Receptor Channel Expressed in *Xenopus* Oocytes

M. Iino[1], S. Ciani[3], K. Tsuzuki[1], S. Ozawa[1], Y. Kidokoro[2]

[1]Department of Physiology, Gunma University School of Medicine, 3-39-22 Showa-machi, Maebashi, 371, Japan
[2]Institute for Behavioral Sciences, Gunma University School of Medicine, 3-39-22 Showa-machi, Maebashi, 371, Japan
[3]Department of Physiology, UCLA School of Medicine, Los Angeles, California, 90024, USA

Received: 3 May 1996/Revised: 25 September 1996

Abstract. Ion permeation properties of the mouse e_2/ζ_1 NMDA receptor channel expressed in *Xenopus* oocytes were studied using the outside-out patch-clamp technique. In symmetrical Na^+ solutions, the single-channel *I-V* relations were almost linear at low electrolyte concentrations, but rectified inwardly for Na^+ concentrations above 50 mM. In symmetrical Na^+ solutions, the ''zero-current conductance'' increased with Na^+ concentration and saturated according to a hyperbolic curve, the half-maximal saturating activity, K_M(Na), being 14.2 mM and the maximal conductance, G_{max}(Na), 53.9 pS. When Ca^{2+} was present with Na^+ in the external solution, the single-channel current was lower than in pure Na^+, although the reversal potential indicated a higher permeability for Ca^{2+} than for Na^+. Using ion activities, P_{Ca}/P_{Na} was found to be about 17. The *I-V* data were fitted with a model based on the Eyring's rate theory, assuming a one-ion pore with three energy barriers and two sites. The K_M(Ca) and G_{max} (Ca) were 76.5 μM and 21.2 pS, respectively. According to the estimated rate constants, K_M for Ca^{2+} is mainly determined by the binding strength of a site located 80% away from the channel opening at the external membrane-solution interface, a position similar to that postulated previously for the Mg^{2+} blocking site.

Key words: NMDA receptor channel — Ion permeation — Current-voltage relation — Eyring-Läuger model — Surface charge — One-ion pore

Introduction

Among the various glutamate receptor channels, the NMDA (N-methyl-D-aspartate) subtype has characteristic ion permeation properties which are suggestive of its role in mechanisms of great physiological importance. Monovalent cations permeate the channel with low selectivity, but major differences exist between Ca^{2+} and Mg^{2+} (Nowak et al., 1984; Mayer & Westbrook, 1987; Ascher & Nowak, 1988). While Mg^{2+} is a potent blocker of the channel, Ca^{2+} is permeant, provided that the pore is in its open state (as a result of agonist binding), and that Mg^{2+} is removed from the permeation pathway. The requirement that both these conditions must be satisfied for Ca^{2+} influx through the NMDA receptor channel, in addition to its demonstrated involvement in the phenomenon of ''long term potentiation'' (Bliss & Collingridge, 1993), has prompted the hypothesis that one of its roles may be that of a ''coincidence detector,'' a device invoked to account for important neurological processes.

It has also been shown that Ca^{2+} ions entering the cell via the NMDA receptor channel are implicated in ''excitotoxicity.'' When cultured neurons were exposed to glutamate in the absence of Mg^{2+} and in the presence of glycine, cells endowed with NMDA receptors died, presumably due to large Ca^{2+} influx. It has been speculated that this type of cell death may occur during certain pathological conditions (Rothman & Olney, 1987).

In view of the great interest for the NMDA receptor channel, it is important to elucidate its ion permeation properties, especially for biological relevant ions such as Na^+ and Ca^{2+}. Using cultured mouse neurons, Ascher & Nowak (1988) studied single-channel currents through the NMDA receptor channel, and demonstrated that substitution of monovalent ions with Ca^{2+} in the external solution causes displacement of the reversal potential in the positive direction, while also decreasing the inward current. Similar effects of Ca^{2+} in the same type of channel were reported later by Jahr & Stevens (1993), who gave also a quantitative description of the data, using a

Correspondence to: Y. Kidokoro

model based on a semi-empirical perturbation approach. More recently, however, Zarei & Dani (1994) have presented a new study of the same channel in cultured mouse neurons, analyzing the conductance at different concentrations of NH_4^+, as well as the permeability ratio between Cs^+, dimethyl-ammonium$^+$ (DMA^+) and Ca^{2+}, using bi-ionic conditions, and exploring a wide range of concentrations for Cs^+ and DMA^+. From the behavior of both the conductance and the bi-ionic potential, they inferred: (i) that the NMDA receptor channel is a one-ion pore, thus arguing against previous claims that the channel may be a multi-ion channel (Mayer & Westbrook, 1987; Ascher & Nowak, 1988; Johnson & Ascher, 1990), and (ii) that only a low surface charge is required to account for few minor deviations from the theoretical predictions of a model for a one-ion pore.

The main purpose of the present study is to evaluate certain basic parameters of the ion permeation properties of the NMDA receptor channel, a goal which in our opinion requires a more systematic analysis of the electrical properties than has been carried out so far. To achieve this goal, the single-channel *I-V* relations were studied first in symmetrical solutions, with Na^+ as the sole permeant ion at different concentrations, and then in solutions where Ca^{2+} was gradually increased in the external medium, while Na^+ was maintained constant and nearly symmetrical on both sides. The questions that we tried to address are of the following type: What are the ''dissociation constants'' and the ''maximal conductance'' of the NMDA-receptor channel, both for Na^+ and for Ca^{2+}? Is it necessary to postulate surface charges to account for the permeation properties of the channel? Assuming validity of the Eyring theory, what is the simplest model capable of giving a good fit to the *I-V* data?

In a wider context, the overall purpose of this study is to build a background of data which will hopefully serve, in conjunction with techniques of molecular biology, to identify the molecular components responsible for the permeation properties of the channel.

The preparation used in this study is the heteromeric mouse ϵ_2/ζ_1 NMDA receptor channel expressed in *Xenopus* oocytes. This receptor channel exhibits properties similar to the native NMDA receptor channel in cultured neurons. For example, L-glutamate and NMDA activate the receptor channel, while neither kainate nor α-amino-3-hydroxy-5-methyl-4-isoxazole propionic acid (AMPA) has any effect. A specific NMDA receptor antagonist, D-2-amino-5-phosphonovalerate (APV), blocks the glutamate responses and so do Mg^{2+} and Zn^{2+} (Kutsuwada et al., 1992). The permeation properties of the expressed ϵ_2/ζ_1 NMDA receptor channel are also very similar to those of the native one. For example, the channel is almost nonselectively permeable to monovalent cations, and is permeable also to Ca^{2+} but is blocked by Mg^{2+} (Tsuzuki et al., 1994). It is thus reasonable to conclude that this is a good model for studying the ion permeation properties of the NMDA receptor channel. Furthermore, due to the absence of other types of glutamate-sensitive ionic pores in this expression system, the NMDA receptor channel events can be identified without ambiguity.

Materials and Methods

Expression of Functional NMDA Receptor Channels in *Xenopus* Oocytes

Capped cRNAs for the mouse NMDA receptor subunit ζ_1 and ϵ_2 were transcribed *in vitro* from linearized plasmids containing appropriate cDNA inserts as described previously (Kutsuwada et al., 1992). Approximately 40 oocytes of *Xenopus laevis* were injected at a time with a mixture of ζ_1 cRNA (13.5 ng per oocyte), and ϵ_2 (19.0 ng per oocyte) and were incubated overnight in Barth's medium (20°C). To remove the follicular membrane, oocytes were treated with 0.5 mg/ml collagenase (Yakult, Tokyo, Japan) for 15-to-30 min at room temperature. Then they were immersed again in Barth's medium (20°C), and were kept there overnight.

Two days after injection, a couple of oocytes from a batch were tested for expression of functional NMDA receptor channels by using the two-microelectrode-voltage-clamp technique. When application of 10 μM L-glutamate and 10 μM glycine evoked inward currents of more than 300 nA, oocytes of the batch were used for single-channel current recording. Shortly before the patch-clamp experiment, an oocyte was immersed in a hypertonic solution for 3 min (Methfessel et al., 1986), and the vitelline membrane was manually removed using a pair of sharp forceps. The ionic composition of the hypertonic solution was (in mM): 280 NaCl, 5 KCl, 1 $CaCl_2$, 25 Tris (pH was adjusted to 7.4 with HCl).

Single-Channel Current Recordings and Current Amplitude Measurements

All recordings were carried out with excised patches in the outside-out mode at room temperature (approximately 25°C) (Hamill et al., 1981). A LIST EPC-7 patch-clamp amplifier was used. Patch pipettes were made from borosilicate glass capillaries and had resistances of about 10 MΩ when filled with the normal internal solution. Single-channel current traces were recorded in a PCM data recorder, and were digitized off-line at the rate of 5 kHz after filtering at 2 kHz.

Measurements of single-channel current amplitudes were carried out using the pClamp software (Axon Instruments, Foster City, CA). Five-to-ten channel events with sufficient durations were measured at each potential level.

Junction potentials were measured or calculated with the Henderson's equation, and the potential levels were corrected accordingly.

Data Fitting and Evaluation of the Parameters

The *I-V* data were fitted to the model using a SIMPLEX minimization algorithm (Press et al., 1988). To give an estimate of the parameters' error, we used an empirical approach, taking into consideration the fact that the dissociation constant, K_M and the maximal conductance, G_{max}, are almost independent of the number of barriers in the model. (For example, a two-barrier model predicted the same values for K_M and G_{max} as our model, even though it fitted the *I-V* data poorly). However, since our three-barrier model depends on five rate constants, there are

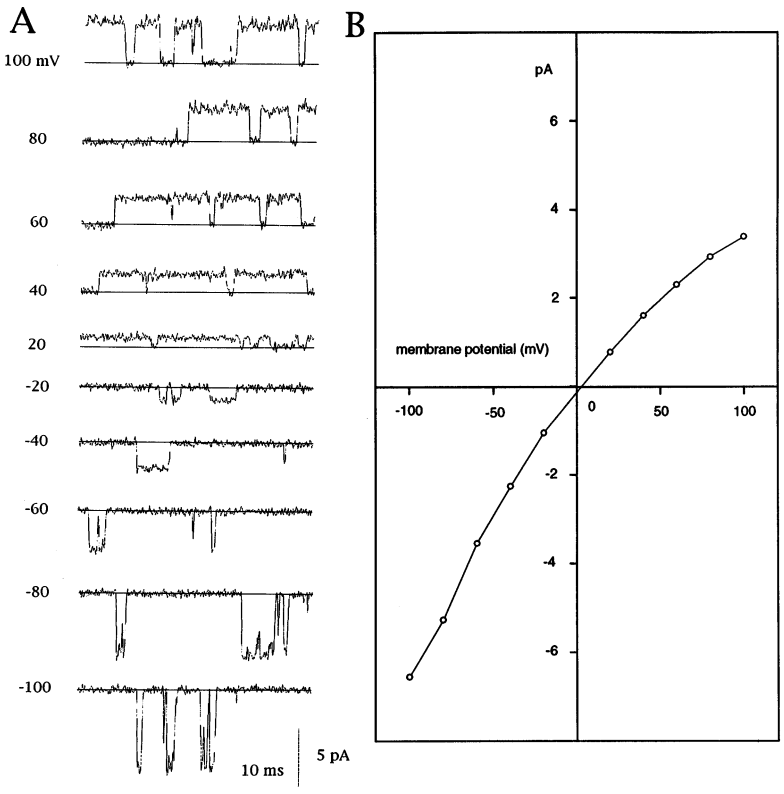

Fig. 1. Single-channel currents induced by 10 μM L-glutamate in the presence of 10 μM glycine. (*A*) sample traces from a representative patch in the outside-out configuration. The bath and the electrode contained the standard external and internal solutions, respectively. The Na^+ concentration was the same on both sides (154.5 mM). Signals were low-pass filtered at 2 kHz (*B*) *I-V* relation obtained from the same patch. The data points were connected by straight lines. The slope conductance was about 50 pS near zero current, but varied with voltage, becoming steeper at negative potentials.

unlimited ways in which these five parameters can be varied without changing K_M and G_{max}. Analyzing a few cases in which three rate constants were changed arbitrarily (the other two being determined by the fixed values of K_M and G_{max}), we found that distortions of the fitting curves became apparent for variations of about 15 to 20% from the optimal values calculated by the computer. Thus, it seems reasonable to infer that a fraction of this order represents a fair estimate of the parameters' relative errors.

Solutions

The ionic compositions of all solutions used in these experiments are listed in Table 1. In all the analyses, ion activities were used instead of concentrations. The activity coefficients of electrolytes were estimated by the formula below (Robinson & Stokes, 1959).

$$\log f = \frac{-A|z_1 z_2|\sqrt{I}}{1+\sqrt{I}} + bI \quad (1)$$

where f denotes the activity coefficient of the electrolyte, I is the ionic strength (in M), while A and b are constants. Following Robinson and Stokes (1959), A was 0.507, and b was 0.161 for NaCl, and 0.20 for $CaCl_2$, z_1 and z_2 are the valences of the two ions of the electrolyte. The activity coefficients of the ions were estimated from those of the electrolytes using of the Guggenheim convention. According to this convention which is based on the Debye-Hückel theory, $f\mathrm{Na} = f_{\mathrm{NaCl}}$, whereas for 2-1 electrolytes such as $CaCl_2$, $f_{\mathrm{Ca}} = (f_{\mathrm{CaCl_2}})^2$ (Butler, 1968; Shatkay, 1968).

Results

When whole cell currents exceeded 300 nA in a few test oocytes upon application of 10 μM glutamate together with 10 μM glycine, oocytes from the same batch were used for single-channel current recordings. Using the outside-out excised patch configuration, single-channel events were observed in the majority of cases when a perfusing solution contained 10 μM glutamate and 10 μM glycine. However, the frequency of channel events tended to decline after several exchanges of the external solutions. Single-channel currents were recorded for membrane potentials ranging from −100 to +100 mV with 20 mV steps. The steady-state current-voltage (*I-V*) relations were thus constructed for various ionic conditions, and were subsequently analyzed using a model based on Eyring's rate theory (Läuger, 1973). Occasionally, substates with lower conductance could be seen, as described previously for the NMDA receptor channel (Cull-Candy & Usowicz, 1987; Jahr & Stevens, 1987; Tsuzuki et al., 1994; Stern et al., 1992), although they appeared rather infrequently. In this study we only dealt with the major conductance state.

I-V Curves in the Symmetrical Distribution of Na^+ Ions

The sample traces in Fig. 1*A* and the *I-V* curve in Fig. 1*B* refer to the case of a patch interposed between symmetrical solutions with 153.8 (117) mM Na^+ (The numbers within parentheses, here and in the rest of the paper, indicate calculated ion activities). Due to technical dif-

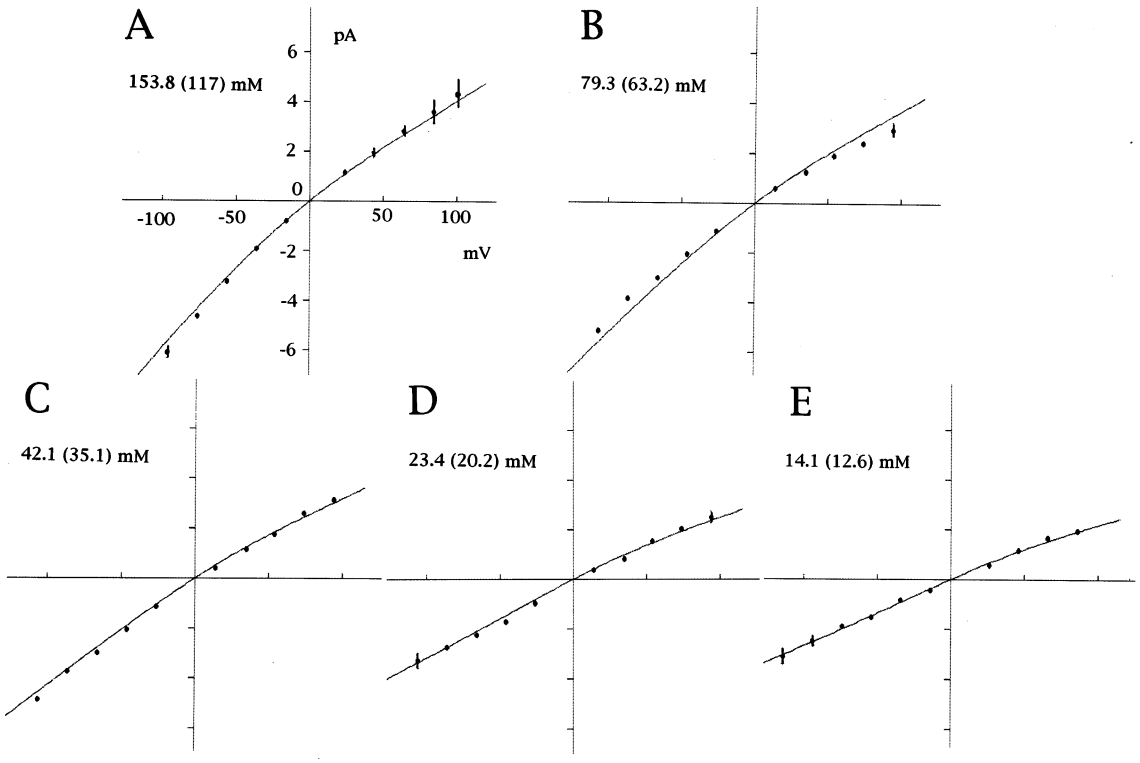

Fig. 2. Single-channel *I-V* relations in symmetrical Na^+ solutions. The five Na^+ concentrations were obtained by diluting the standard solution (solution 1) and using sucrose (solution 3) to maintain osmolarity. Results from various experiments were pooled for 153.8 (117) mM ($n = 3$, number of patches examined), 79.3 (63.2) mM ($n = 5$), 42.1 (35.1) mM ($n = 7$), 23.4 (20.2) mM ($n = 6$) and 14.1 (12.6) mM ($n = 5$), the numbers within parentheses being the estimated activities for Na^+. Smooth lines are fits to the data with Eq. (A5). The rate constants for Na^+, divided by 10^9 and listed in the order: $\overline{\rho'}_{Na}$ (s^{-1} M^{-1}), $\overline{\lambda'}_{Na}$ (s^{-1}), $\overline{\mu'}_{Na}$ (s^{-1}), $\overline{\rho''}_{Na}$ (s^{-1} M^{-1}), $\overline{\lambda''}_{Na}$ (s^{-1}), $\overline{\mu''}_{Na}$ (s^{-1}), are: 1.48, 0.17, 0.028, 1.39, 0.072, 0.070. The electrical distances, defined in Fig. 8*A*, are: $\alpha = 0.23$, $\beta = 0.54$, $\gamma = 0.23$. Note that since the rate constants are related by ''microscopic reversibility'' (Eq. (A4)), and since the sum of the three electrical distances is one, the number of independent parameters is seven (and not nine as it may seem at first sight from the list above).

ficulties of forming stable patches in zero Ca^{2+}, this ion was not buffered in the external solution, although its concentration was measured in nominal Ca^{2+}-free solutions, and was found to be approximately 0.55 μM. Despite the symmetry of the ion composition, the *I-V* relation in the Fig. 1*B* is neither symmetrical nor linear, the slope conductance being somewhat steeper when the current flows in the inward direction.

The zero-current channel conductance in the experiments shown in Fig. 1*B* (pooled data at 153.8 (117) mM Na^+ concentration) was estimated by connecting the points at −10 and +10 mV, and was found to be about 50 pS. This value is identical to that reported previously (50 pS) by Tsuzuki et al. (1994), who performed the measurement in solutions with the same Na^+ concentration, but with 1 mM Ca^{2+} in the bath. The similarity between these two data, despite the known blocking effect of Ca^{2+} on the current (*see* Fig. 4), is probably due to two compensating features: inhibition by Ca^{2+}, and the fact that Tsuzuki et al. (1994) took their measurements at potentials between −40 and −60 mV, a region where the slope of the *I-V* curve, as we noted above, is steeper than near zero current.

To study the effects of ion concentration, a family of *I-V* curves was obtained by reducing the Na^+ concentration symmetrically on both sides of the patch and maintaining isotonicity by replacing Na^+ with sucrose (Fig. 2). Note that in this series of five experiments the ionic strength of the solutions was not constant, but varied in parallel with the Na^+ concentration. (The external Na^+ concentration was reduced by mixing solution 1 and 3, and the internal Na^+ concentration was reduced by mixing solution 6 and 7 in Table 1). In none of the five cases are the *I-V* curves rigorously linear, although they become more straight at low ion concentrations. As is shown in Fig. 3, the zero-current conductance increases with Na^+ activity, and eventually saturates at a limiting value, (G_{max}), estimated to be approximately 54 pS. Although it was difficult to perform accurate measurements at very low Na^+ concentrations, the data in Fig. 3 suggest that, as the Na^+ concentration decreases, the channel conductance declines following a regular Mi-

Table 1. Composition of solutions

External solutions	NaCl	NaF	$CaCl_2$	Sucrose	HEPES* −NaOH	EGTA
(1) Standard Na^+	150	0	0	0	10	0
(2) Ca^{2+}	0	0	100	0	10	0
(3) Sucrose	0	0	0	260	10	0
(4) Na^+-sucrose	100	0	0	86	10	0
(5) Na^+-Ca^{2+}	100	0	30	0	10	0
Internal solutions						
(6) Standard	48	100	0	0	10	1
(7) Sucrose	0	0	0	260	10	1

* 4.5 mM NaOH was needed to adjust pH to 7.4

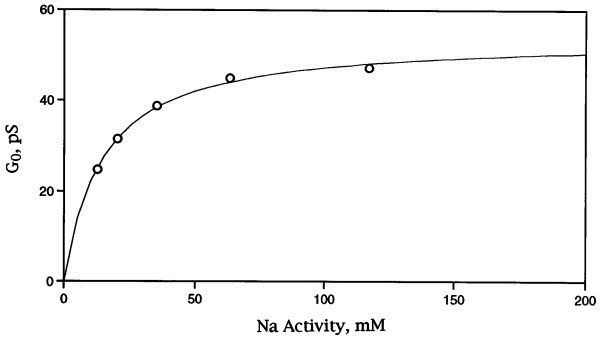

Fig. 3. Conductance-activity relation for Na^+. The five conductance values were determined from the data in Fig. 2. The measured zero-current conductances were 50 pS for 154.5 (117) mM Na^+, 46.1 pS for 79 (63.2) mM Na^+, 40.2 pS for 42.1 (35.1) mM Na^+, 33.2 pS for 23.4 (20.2) mM Na^+ and 26.5 pS for 14.1 (12.6) mM Na^+. The continuous curve is drawn according to Eq. (2), with K_M = 14.2 mM and G_{max} = 54 pS. These values were not deduced from an independent fit, but were obtained by substituting in Eq. (3) and (4) the rate constants listed in the legend of Fig. 2.

chaelis-Menten curve with a K_M of about 14.2 mM. According to the Gouy-Chapman theory, this simple behavior would not be expected if a significant surface charge were present on both sides of the channel (a surface charge being designated ''large'' when it generates a surface potential greater than RT/F, 25 mV, in solutions with physiological ionic strength). However, as we shall see later in the Discussion, an asymmetrical distribution of surface charges with a significant charge present only on one side of the channel cannot be easily excluded.

Interaction between Ca^{2+} and Na^+ Ions

The sample traces in part *A* of Fig. 4 refer to single-channel currents for an outside-out patch interposed between an external solution containing a mixture of 104.5 (78.5) mM Na^+ and 30 (8.6) mM Ca^{2+} (solution 5 in Table 1), and an internal solution of 153.1 (117) mM Na^+ (solution 6 in Table 1). The corresponding *I-V* relation is given by the dotted curve in Fig. 4*B*, where, for comparison we plotted also an *I-V* curve obtained with 0 Ca^{2+} and 153.8 (117) mM Na^+ (solution 1 and 6 in Table 1) on both sides of the patch. Figure 5 illustrates the effect of gradually varying the Ca^{2+} concentration in the external bath from 0.3 (0.1) mM (Fig. 5*E*) to 30 (8.6) mM (Fig. 5*A*). (The intermediate concentrations of Ca^{2+} were prepared by mixing solution 4 and 5 in Table 1). The continuous lines are the theoretical fitting curves obtained with the model. As one can see, the reversal potential shifts to the right, indicating a high permeability to Ca^{2+}, a result similar to that shown previously by Ascher & Nowak (1988) in cultured mouse neurons, and also by Tsuzuki et al. (1994) in the same preparation as that studied in this paper. In Fig. 6, the reversal potential is plotted *vs.* the calcium activity in the bath; the smooth line is the fit to the data with Eq. (12). The estimated permeability ratio, P_{Ca}/P_{Na}, was about 17, a value considerably higher than that reported previously (6.2 Iino, Ozawa & Tsuzuki, 1990; 3.6, Tsuzuki et al., 1994). Probably, the main reason for the discrepancy lies in that we used ion activities instead of concentrations. In fact, by using Eq. (1) to estimate the activity coefficient of the electrolyte, and then the Guggenheim convention to calculate the ion activities, one finds Ca^{2+} activities that are much smaller than the respective concentrations. For example, in a mixture of 30 mM $CaCl_2$ and 100 mM NaCl, the estimated Ca^{2+} activity is only 8.6 mM. Using activity coefficients, also Mayer & Westbrook (1987) reported a relatively high value for P_{Ca}/P_{Na} in cultured mouse neurons, (P_{Ca}/P_{Na} = 10.2).

The amplitude of both inward and outward currents decreased as the external Ca^{2+} concentration increased. Similar effects of external Ca^{2+} on the *I-V* curves were observed in the glutamate receptor channel from cultured embryonic *Drosophila* myotubes (Chang, Ciani & Kidokoro, 1994). The two apparently conflicting effects described above: the inhibitory effect of Ca^{2+} on the Na^+

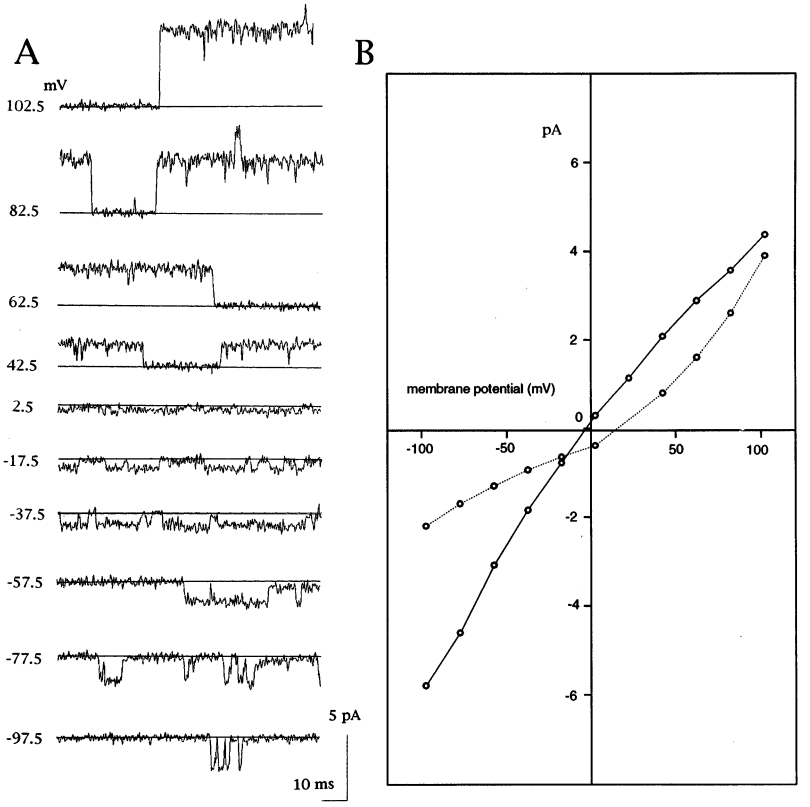

Fig. 4. Single-channel current-voltage relation in the presence of external Ca^{2+}. (*A*) sample tracings from an outside-out patch exposed to an external solution containing a mixture of 30 mM $CaCl_2$ and 100 mM NaCl (solution 5 in Table 1). The solution in the pipette was the standard internal solution (solution 6 in Table 1). (*B*) *I-V* relation corresponding to the traces shown in *A*, and *I-V* curve in symmetrical Na^+ (154.5 mM) and 0 Ca^{2+} (solution 1 in Table 1), shown here for comparison.

current, and the ability of Ca^{2+} to shift the reversal potential in the direction of positive voltages with a permeability higher than that of Na^+, are perfectly compatible with models for ''one-ion'' channels based on the Eyring-Läuger theory, while they are inconsistent with the classic result obtained by integration of the Nernst-Planck equation assuming constant field.

A ''Three-barrier, One-ion'' Model for the NMDA Receptor Channel

I-V Relations

The experiments of Zarei and Dani (1994) suggest that the NMDA receptor channel behaves as a one-ion pore, at least for some permeant ions, Na^+ and Ca^{2+} included. Complying with this suggestion, and applying the Eyring-Läuger theory for singly occupied pores (Läuger, 1973), we have found that a ''two site, three barrier'' model, similar to that described previously for a glutamate receptor channel in *Drosophila* (Chang et al., 1994), gave a good fit to the *I-V* data for the NMDA receptor channel. A simpler ''one site, two barrier'' model for the channel was also tested, but, as we discuss later, was found to be much less satisfactory. We have thus pursued our analysis using the slightly more complex kinetic scheme with two internal sites and three barriers. It should be intuitively clear that, in the presence of only one permeant ion species, this model is characterized by three states of occupancy: the empty state and two occupied states, with the ion located in either of the two available sites. It is also obvious that there will be two additional states (and thus a total of five) when the permeant ion species are two, as in the case of mixtures of Na^+ and Ca^{2+} (*see also* Fig. 8*B* in the Appendix). Using well-known methods (Läuger, 1973; *see also* Appendix), one easily obtains explicit expressions for the ion fluxes and the current as functions of membrane voltage and ion concentrations. For simplicity, we used the assumption that the barrier peaks are halfway between successive sites. With this assumption, and in the case of only one permeant ion, the model has seven independent parameters: two independent electrical distances and five independent rate constants. In fact, although three distances: α, β, γ, and six rate constants, ν', λ', μ', ν'', λ'', μ'', appear in Fig. 8, the former are subject to the condition that their sum is equal to one, while the latter are related by the condition of ''microscopic reversibility,'' given by Eq. (A4) in the Appendix. Equation (A5), which refers to the case of only one permeant ion, was used to fit the data in Fig. 2. The five single-channel *I-V* curves in this figure correspond to five different symmetrical concentrations of Na^+, this being the only permeant ion in the solutions. The rate constants that optimized the fit to the *I-V* relations in Fig.

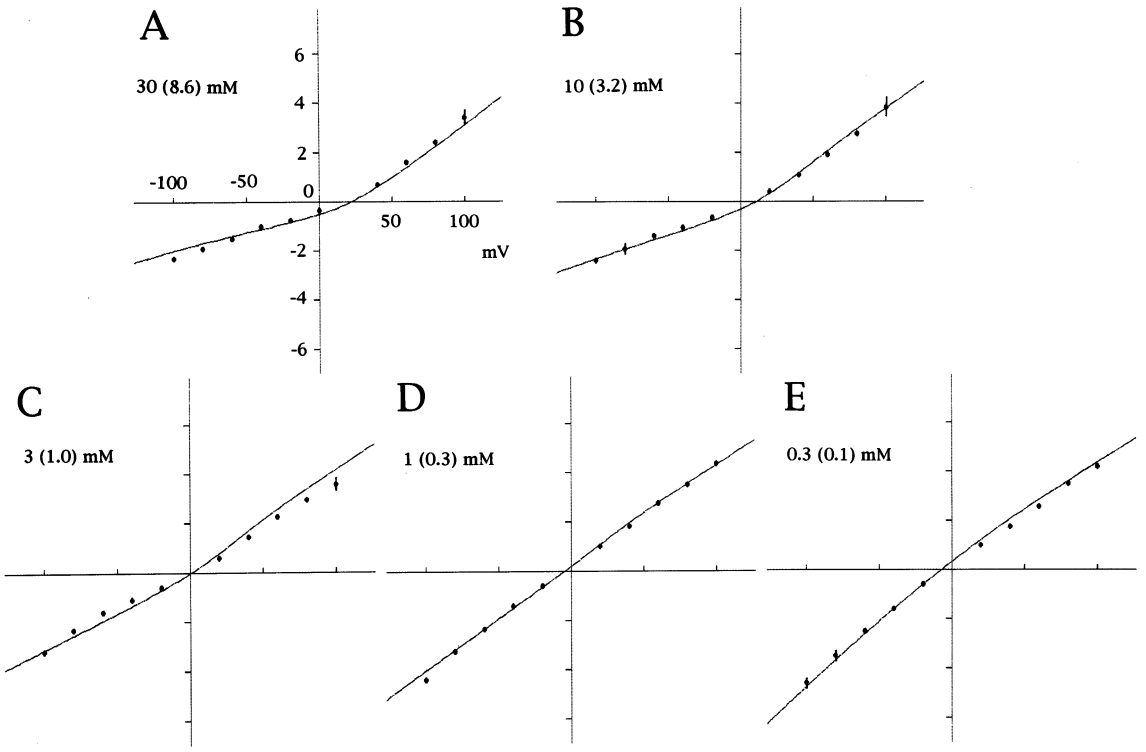

Fig. 5. Single-channel *I-V* relations for Ca^{2+}-Na^+ mixtures in the external medium. The external Na^+ concentration was 104.5 mM, while the external Ca^{2+} concentration ranged from 0.3 to 30 mM. The solution in the pipette was the standard internal solution (solution 6 in Table 1). Results from different patches are pooled for 30 (8.6) mM Ca^{2+} ($n = 4$), 10 (3.2) mM Ca^{2+} ($n = 3$), 3 (0.83) mM Ca^{2+} ($n = 3$), 1 (0.33) mM Ca^{2+} ($n = 6$), 0.3 (0.11) mM Ca^{2+} ($n = 6$), the numbers within parentheses being the estimated activities for Ca^{2+}. These solutions were prepared by mixing solution 4 and 5 in Table 1. The continuous curves represent fits to the data with Eq. (A9), all the rate constants for Na^+ having been fixed at the values estimated previously, and listed in the legend of Fig. 2. The fitting rate constants for Ca^{2+}, divided by 10^9, and given in the same units and order as those in the legend of Fig. 2 are: 26.5, 0.060, 0.0076, 19.3, 0.25, 0.0025.

2 are listed in the corresponding figure legend. These values were then substituted in the equation for the current in mixtures of two ions, Eq. (A9), which was used to fit the *I-V* data in Na^+-Ca^{2+} mixtures (Fig. 5), and thus to deduce the rate constants for Ca^{2+}. In the experiments with Na^+-Ca^{2+} mixtures, Na^+ was maintained constant, while Ca^{2+} was varied from 0.3 to 30 mM in the external solution. The *I-V* data in Na^+-Ca^{2+} mixtures, together with the fitting curves obtained using Eq. (A9), are shown in Fig. 5, and the calculated rate constants for Ca^{2+} are given in the corresponding figure legend.

Zero-voltage Conductance and Permeability Ratio

When only one permeant ion is present in the two solutions at the same concentration, it can be shown, using Eq. (A5), that the channel conductance in the limit of zero current becomes:

$$G_0 = G_{\max} \frac{a}{a + K_M} \tag{2}$$

where K_M, the dissociation constant of the permeant ion from the channel, and $G_{\max}$, the maximal conductance, can be expressed in terms of the rate constants by the following equations,

$$K_M = \frac{\overline{\mu'}\,\overline{\mu''}}{\overline{\rho'}\,\overline{\mu'} + \overline{\rho''}\,\overline{\mu''}} \tag{3}$$

$$G_{\max} = \frac{z^2e^2}{kT} \frac{\overline{\lambda'}\,\overline{\lambda''}}{(\overline{\lambda'} + \overline{\lambda''})(\overline{\lambda}/\overline{\mu''} + \overline{\lambda''}/\overline{\mu'} + 1)} \tag{4}$$

The meaning of the rate constants in the above equations should be clear from inspection of Fig. 8 (*see also* the Appendix), and the bar on top is used to denote the values of the rate constants at zero voltage. Substituting the numerical values for the rate constants given in the legends of Fig. 2, one finds: K_M(Na) = 14.2 mM and $G_{\max}$(Na) = 53.9 pS. A plot of the ''zero current'' conductance is exhibited in Fig. 3. Note that the continuous curve in Fig. 3 is not an independent fit of the conductance data with Eq. (2), but is just the theoretical plot of

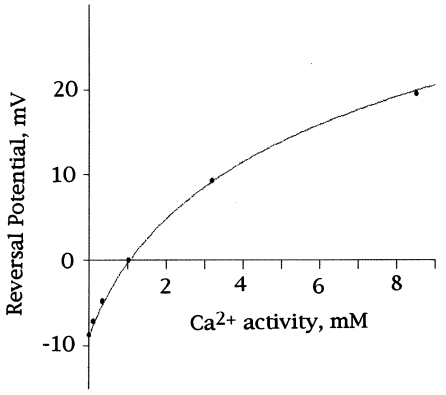

Fig. 6. Dependence of reversal potential on Ca^{2+} activity. The reversal potentials were estimated by linear interpolation, using the data equivalent to those shown in Fig. 5 at each Ca^{2+} concentration. They were −8.7 mV for 0 mM Ca^{2+}, −7.2 mV for 0.3 (0.11) mM Ca^{2+}, −4.8 mV for 1 (0.33) mM Ca^{2+} 0 mV for 3 (0.83) mM Ca^{2+}, 9.2 mV for 10 (3.2) mM Ca^{2+} and 19.5 mV for 30 (8.6) mM Ca^{2+}. The continuous curve represents the fit to the data with Eq. (12). The estimated permeability ratio was 17.

Eq. (2), using the calculated numbers for K_M and G_{max} reported above. The corresponding K_M and G_{max} for Ca^{2+}, deduced by substitution of the constants listed in Fig. 5 in Eqs. (3) and (4), are: $K_M(Ca) = 76.5$ μM and $G_{max}(Ca) = 21.2$ pS. Due to obvious experimental restrictions, one cannot measure the channel conductance in pure Ca^{2+} solutions, and thus test the accuracy of the values for K_M and G_{max} in the same way as it was done with Na^+. However, as we shall see, a less direct, but still valuable test for consistency can be obtained by comparing the measured permeability ratio, P_{Ca}/P_{Na}, determined empirically using the constant field theory with its theoretical expression in terms of K_M and G_{max} (*see* Eq. 8).

As can be seen from Eq. (A9), in models for channels based on the Eyring-Läuger theory, the permeability ratio generally depends on the voltage across the membrane. To obtain an explicit expression for P_{Ca}/P_{Na}, it is convenient to define the quantity:

$$Q_{Na}(\phi) = \exp\left(z_{Na}(\gamma - \alpha)\frac{\phi}{2}\right) + \frac{\overline{\lambda''}_{Na}}{\overline{\mu'}_{Na}}\exp\left(-z_{Na}(\alpha+\beta)\frac{\phi}{2}\right) + \frac{\overline{\lambda'}_{Na}}{\overline{\mu''}_{Na}}\exp\left(z_{Na}(\beta+\gamma)\frac{\phi}{2}\right) \quad (5)$$

ϕ is the voltage in units of *RT/F*, and the meaning of the rate constants, $\overline{\lambda}$, $\overline{\mu}$, as well as that of the ''electrical'' distances, α, β, γ, are given in the Appendix, but can also be guessed from inspection of Fig. 8. Defining a similar quality, Q_{Ca} for Ca^{2+}, the permeability ratio can be written in the form

$$\frac{P_{Ca}}{P_{Na}} = \left(\frac{p_{Ca}}{P_{Na}}\right)_0 F(\phi) \quad (6)$$

where $F(\phi)$ is

$$F(\phi) = \frac{Q_{Na}(\phi)Q_{Ca}(0)}{Q_{Na}(0)Q_{Ca}(\phi)} \quad (7)$$

and $(P_{Ca}/P_{Na})_0$, the permeability ratio near zero voltage, is given by

$$\left(\frac{P_{Ca}}{P_{Na}}\right)_0 = \frac{z_{Na}^2}{z_{Ca}^2}\frac{G_{max}(Ca)}{G_{max}(Na)}\frac{K_M(Na)}{k_M(Ca)} \quad (8)$$

By substituting in Eq. (8) the numerical values of K_M and G_{max}, both for Na^+ and Ca^{2+}, one finds $(P_{Ca}/P_{Na})_0 = 18$. As we shall see later, a similar value is obtained by fitting the reversal potential with an equation deduced from the ''constant field'' theory. Using Eq. (3) and (4), and recalling the condition for ''microscopic reversibility'' given by Eq. (A4), Eq. (8) can also be written,

$$\left(\frac{P_{Ca}}{P_{Na}}\right)_0 = \frac{z_{Na}^2}{z_{Ca}^2}\frac{\overline{\rho''}_{Ca}\,\overline{\lambda''}_{Ca}\,\overline{\mu''}_{Na}}{\overline{\rho'}_{Na}\,\overline{\lambda'}_{Na}\,\overline{\mu'}_{Ca}}\frac{Q_{Na}(0)}{Q_{Ca}(0)} \quad (9)$$

Expressing the rate constants in terms of the energy barriers, (*see Eq.* (A1)), it could be shown that Eqs. 6 to 9, and thus the permeability ratios, are independent of the energy levels of the internal sites. This important feature is somehow hidden in the otherwise useful expression for $(P_{Ca}/P_{Na})_0$ given by Eq. (8), since it may not be obvious that the energy levels of the internal sites cancel out in the ratio G_{max}/K_M. Although P_{Ca}/P_{Na}, as given by Eq. (6), depends on the membrane voltage, it can be shown that its value remains very close to $(P_{Ca}/P_{Na})_0$ for membrane potentials within the range of those measured in our experiments (−5 to 20 mV).

Discussion

A previous study of the NMDA receptor channel in cultured CA1 hippocampal neurons reported measurements of the single-channel conductance using NH_4^+, as well as measurements of bi-ionic potentials in the presence of Cs^+, DMA^+ (dimethyl-ammonium) and Ca^{2+} (Zarei & Dani, 1994). From the behavior of the conductance-concentration curve, and from the constancy of the bi-ionic potential when the ion concentrations were changed by proportional amounts in the solutions, it was argued that the channel behaved as a one-ion pore. Minor deviations from the theory could be accounted for by

postulating a small surface charge near the opening of the channel (equivalent to 0.0002 electronic charges/Å^2). These experiments are clearly important, because they provide relevant information about the channel without using specific models and assumptions.

The data in this paper extend those of previous studies by describing the single-channel current in a wide range of voltages and concentrations, and using physiologically important ions such as Na^+ and Ca^{2+}. However, in contrast to the type of the measurements mentioned above (bi-ionic potentials and conductance *vs.* concentration at constant voltage), a quantitative analysis of the *I-V* relationships requires the use of a specific model. The simplest kinetic scheme that gives a satisfactory fit to our data is a one-ion model with two sites and three barriers, based on the Eyring-Läuger theory, and quite similar to a model used previously for studying a different glutamate receptor channel in *Drosophila* (Chang et al., 1994). Although it would be unrealistic to claim uniqueness with this type of model (since, for example, models with more than three barriers would probably also fit the data), it seems however reasonable to expect that some basic information about the permeation properties may be deduced by fitting the data with the simplest kinetic scheme that proves to be adequate. An even simpler model with only one site and two barriers was also tested. Although it gave similar values for K_M and G_{max}, it predicted supralinear *I-V* curves in the region of measurable high voltages, a feature that is not observed in the data.

The Channel Conductance in Pure Na^+ Solutions

The continuous curves in Fig. 2, drawn according to Eq. (A5), represent theoretical fits to the *I-V* data for the case in which Na^+ was the only permeant ion present. The curves are fairly symmetrical at low Na^+ concentrations, but show some inward rectification at higher concentrations. As one can deduce from the fitting values of the rate constants (*see* the legend of Fig. 2), the rectification is related to the unequal depths of the two internal sites. In fact, denoting by $\overline{K'_d}(=\overline{\mu''}/\overline{\rho'})$ the dissociation constant of the site close to the internal membrane interface, and by $\overline{K''_d}(=\overline{\mu'}/\overline{\rho''})$ that of the site close to the external interface, one finds 48.7 mM for $\overline{K'_d}$ and 20.1 mM for $\overline{K''_d}$. On the other hand, at sufficiently low Na^+ concentrations (and thus low occupancy, a condition in which the current-voltage characteristics are expected to be independent of the depth of the energy wells), the symmetry of the *I-V* curves is consistent with the fact that peaks of the two lateral energy barriers have almost equal height. In fact, $\overline{\rho'} = \overline{\rho''}$, as one can see in the legend of Fig. 2.

Figure 3 shows that the saturation of the ''conductance-activity'' curve is well described by a Michaelis-Menten type of equation, such as Eq. (2) where K_M and G_{max} have been estimated by substituting in Eqs. (3) and (4) the appropriate rate constants listed in the legend of Fig. 2. As we shall discuss later, the features of this curve argue against the presence of a large surface charge on both sides of the channel.

Na^+-Ca^{2+} Interaction

Except for the absolute value of the current, the properties of the *I-V* relations in Na^+-Ca^{2+} mixtures are quite similar to those of the glutamate receptor channel of *Drosophila* (Chang et al., 1994). Ca^{2+} has an inhibitory effect on the current, even though its permeability is higher than that of Na^+. While incompatible with the classic constant-field theory, these two features are quite consistent with models for ''one-ion'' pores based on the Eyring-Läuger theory. This can be seen in Fig. 5, where the smooth curves represent a fit to the data using our model which is based on that theory. More specifically, the equation used was Eq. (A9), in which all the parameters for Na^+ were fixed at the values deduced previously by fitting the data in Fig. 2. As in the case of the glutamate receptor channel of *Drosophila*, the shift of the reversal potential observed upon changing the external Ca^{2+} concentration could be accounted for by the high permeability of the channel to Ca^{2+} ions.

A Comparison between P_{Ca}/P_{Na} Estimated from the Eyring Model and the Constant Field Equation

Interestingly, it was found that the classic constant-field theory describes very well the dependence of the reversal potential on Ca^{2+} activity, despite its manifest inability to account for the *I-V* relations. Moreover, the value estimated for the permeability ratio, P_{Ca}/P_{Na} ($=17$), is very close to that obtained using the Eyring model ($=18$). The similarity between these two values is not circumstantial, but can be justified by the following considerations. Using Eq. (A9) for the *I-V* relation in Na^+-Ca^{2+} mixtures (which is derived from the Eyring model), and imposing the condition of zero current, one finds:

$$\frac{P_{Ca}}{P_{Na}} = \frac{[a'_{Na}\exp(^{3\Phi}/_2) - a''_{Na}\exp(^{\Phi}/_2)]}{2a''_{Ca}} \qquad (10)$$

where the left-hand side is defined in Eqs. (6–8). Note that Eq. (10) cannot be solved explicitly for ϕ or V, mainly because of the complex voltage-dependence of P_{Ca}/P_{Na}. Moreover, even if P_{Ca}/P_{Na} could be considered almost constant in the range of measured potentials, (as is the case in our experiments: −5 to 20 mV), Eq. (10) would still be a cubic equation in $\exp(\phi/2)$, and thus it would be impractical to solve it for ϕ. However, using

the Nernst-Planck equation, and extending the ''constant-field'' theory to mono-divalent mixtures, it can easily be shown (*see* Appendix) that the counterpart to Eq. (10) is:

$$\frac{P_{Ca}}{P_{Na}} = \frac{[a'_{Na}\exp(^{3\Phi}/_{2}) - a''_{Na}\exp(^{\Phi}/_{2})]}{2a''_{Ca}}\cosh(^{\Phi}/_{2}) \qquad (11)$$

The main difference between Eqs. (11) and (10) is the quantity $\cosh(\phi/2)$ which appears in Eq. (11). However, since $\cosh(\phi/2)$ remains close to one between −5 and 20 mV, Eqs. (10) and (11) are interchangeable in that range, implying that similar values for P_{Ca}/P_{Na} will be obtained from the two theories. The practical advantage of Eq. (11) is that it can be solved analytically for *V*, thus yielding an explicit expression for the reversal potential as a function of the permeability ratio and the ion activities. The result is:

$$V = \frac{RT}{F}\ln\left\{\frac{a''_{Na}}{2a'_{Na}} - \frac{1}{2} + \sqrt{\left(\frac{a''_{Na}}{2a'_{Na}} + \frac{1}{2}\right)^2 + 4\frac{P_{Ca}a''_{Ca}}{P_{Na}a'_{Na}}}\right\} \qquad (12)$$

Although we derived Eq. (12) independently, it was called to our attention that it is a particular case of a more general result obtained by Spangler (1972). As is shown in Fig. 6, Eq. (12) gives a good fit to the data with a permeability ratio equal to 17. This number is very close to that calculated by substituting in Eq. (8) the values for K_M and G_{max} deduced by fitting the *I-V* data with our model (*see* Table 2).

The notion that in the ''constant-field'' theory the equation for the reversal potential is more general than the equation for the current has already been emphasized previously (e.g., Hille, 1984). However, while past discussions generally referred to mixtures of monovalent cations, here we have the example of an important system in which similar considerations hold true also for mixtures of monovalent and divalent cations.

Effects of Surface Charges

To discuss possible effects of the surface charges on our measurements, we will consider separately the cases of symmetrical and asymmetrical surface charges.

Symmetrical Surface Charges

As we mentioned before, the behavior of the conductance in Fig. 3 suggests that it is unlikely that a large surface charge is present on both sides of the channel. According to the Gouy-Chapman theory, if a negative charge is present at the membrane surface, decreasing the ionic strength in the adjacent solution will cause the surface potential to diverge to highly negative values, while the ion concentrations at the interface will remain finite (*see* e.g., McLaughlin, 1989). Thus, if a surface charge is present at both interfaces, and if the effects of the surface potential extend to the region near the mouth of the channel, also the channel conductance will tend to remain finite at low ionic strengths in the solutions. Although it was difficult to measure the conductance at very low Na^+ concentrations, the points in Fig. 3 do not suggest this type of behavior. On the basis of these concepts, we have previously formulated a theoretical criterion to estimate an upper limit for the charge density, σ_{max1} that may be present at the membrane-solution interfaces, even when conductance data at very low concentrations are not available (Chang et al., 1994). The main results can be thus summarized: If the charge density, is given in electron charges/Å^2, and the dissociation constant, K_M, in moles/liter (M), one finds

$$\sigma_{max} < \frac{1}{272}\left\{K_M G_{int}/(G_{max} - G_{int})\right\}^{1/2} \qquad (13)$$

where G_{max} is the maximal conductance defined in Eq. (4), and G_{int} is the intersection with ordinate axis (*G*-axis) of the straight-line tangent to the curve in Fig. 3, drawn from any of its points. Although inequality (13) holds true for G_{int} values obtained from the tangents to any point of the curve, the best estimates for σ_{max} will be obtained using straight-line tangents drawn from points corresponding to the lowest conductance experimentally available. Applying this criterion to the data in Fig. 3, one finds approximately: $G_{int} = 15$ pS, and, using relation (13)

$$\sigma_{max} < 0.00024 \text{ electron charges/Å}^2 \qquad (14)$$

which is a value very close to that estimated by Zarei & Dani (1994). Allowing for the presence of this small charge density in our model, we found negligible changes in the values of the fitting rate constants.

It is important, however, to recognize that the discussion given above is valid only if the charge is distributed symmetrically on both interfaces, the situation being instead quite different if the charge is present only (or predominantly) at one interface.

Asymmetrical Surface Charge

For simplicity (but without any loss of generality with respect to the point that we wish to make), we shall now consider a simpler ''two-barrier'' model with one internal site, and will assume, for example, that a negative surface charge exists only at the interface with the external solution. In a ''two-barrier'' model, the kinetics is described by four rate constants, only three of which are

Table 2. Parameters of the model

	K_d'	K_d''	K_M	G_{max}	$(P_X/P_{Na})_{exp}$	$(P_X/P_{Na})_{0(theor)}$
	(mM)	(mM)	(mM)	(pS)		
Na^+	48.7	20.1	14.2	54	1	1
Ca^{2+}	0.094	0.49	0.076	21.2	17	18

Fitting values for the ''dissociation constants'' of the two sites. K_d' ($=\overline{\mu''}/\overline{\rho'}$), K_d'' ($=\overline{\mu'}/\overline{\rho''}$), the overall ''dissociation constant'' of the channel, $K_M(=K_d'K_d''/(K_d' + K_d''))$, the maximal conductance, G_{max}, and the permeability ratio, $(P_{Ca}/P_{Na})_{exp}$, is the value calculated by fitting the data of Fig. 6 with Eq. (12); $(P_{Ca}/P_{Na})_{0(theor)}$ is the theoretical value calculated using Eq. (8).

however independent due to ''microscopic reversibility'' ($\overline{\rho'}\,\overline{\mu'} = \overline{\rho''}\,\overline{\mu''}$), and by two electrical distances, α and β, subject to the obvious condition that $\alpha + \beta = 1$. Using ion concentrations instead of activities defining K_M by $\overline{\mu'}/\overline{\rho''}$ ($=\overline{\mu''}/\overline{\rho'}$), and denoting the surface potential by ϕ_S, it is shown in the Appendix that, in the case of a single type of monovalent permeant cation at the same concentration in the two solutions, the ''zero-current'' conductance is given by:

$$G_0 = \frac{(F^2/RT)\,\overline{\rho''}C\exp(-\phi_s/2)}{\exp(\alpha\phi_s/2) + \frac{\overline{\mu'}}{\overline{\mu''}}\exp(-\beta\phi_s/2) + \frac{C}{K_M}\left[\exp(-\alpha\phi_s/2) + \frac{\overline{\mu'}}{\overline{\mu''}}\exp\{(\beta - 2)\phi_s/2\}\right]} \quad (15)$$

As is well known from the Gouy-Chapman theory (e.g., *see* McLaughlin, Szabo & Eisenman, 1971), if only one monovalent electrolyte is present (e.g., NaCl), the surface potential is expected to vary with the electrolyte concentration, C, according to the equation:

$$\exp(-\phi_s) = 1 + A/2C + \left[A/C + A^2/4C^2\right]^{1/2} \quad (16)$$

where A depends on the surface charge density, σ, and the temperature, T. If T is room temperature, if C is expressed in moles/liter (M), and if the surface charge density, σ, is given in electron charges/Å^2, the numerical value of A is

$$A = (272\sigma)^2 \quad (17)$$

With the aid of Eq. (16) and (17) it can be easily proved that G_0, given by Eq. (15), decreases with C as a power function of C, with a positive exponent generally smaller than one. For example, considering a symmetrical ''two-barrier'' channel, so that $\overline{\mu'} = \overline{\mu''}$ and $\alpha = \beta = \frac{1}{2}$, and assuming that the permeant ion is monovalent, it can be shown (*see* Appendix) that at low ion concentrations Eq. (15) becomes approximately:

$$G_0 = (F^2/RT)\,\overline{\rho'}A^{1/4}C^{3/4} \quad (18)$$

Thus, G_0 decreases to zero with C as the 0.75th power of C, regardless of the value of the surface charge density. A qualitatively similar behavior can be seen in Fig. 7, where the same data of Fig. 3 are fitted using Eq. (15), and assuming the presence of a negative surface charge density on the external interface of 0.002 electron charges/Å^2. This value is 10 times larger than the charge density estimated using criterion (13) for the ''maximal'' symmetrical surface charge density (*see* relation 14). In the physical situation that corresponds to Fig. 7, there would be a large negative surface potential at the external surface, the Na^+ concentration at that interface would be much greater than in the bulk solution, and K_M would be 30 mM, twice as large as computed from our model with no surface charges.

Thus, Fig. 7 shows that the same data that in Fig. 3 are well described by a model without surface charges, can also be fitted with a model with a relatively large surface charge at one interface (0.002 electron charges/Å^2). It may be worth emphasizing again that it would be impossible to fit the data of Fig. 3 or Fig. 7 with a similar charge at both interfaces.

Although at present there is no compelling reason for preferring a model with asymmetrical surface charges to the simpler one described in this paper (also because it would be difficult, with that model, to fit the symmetrical *I-V* data of Fig. 2 at low Na^+ concentration), the above considerations suggest that some caution is appropriate when drawing conclusions about surface charges from the conductance *vs.* concentration plot. In particular, even when it is found that the conductance tends to zero with the ionic strength, the presence of a surface charge at one of the two interfaces cannot be excluded.

The cDNAs for ζ_1 and ϵ_2 were the gift of Professor Masayoshi Mishina, Department of Pharmacology, University of Tokyo. We thank Dr. Hiroshi Kuromi for helping us by measuring Ca^{2+} concentrations in our nominally Ca^{2+}-free solutions.

This research was supported by a grant from the Mitsubishi foundation and grants-in-aid from the Ministry of Education, Science, Sports and

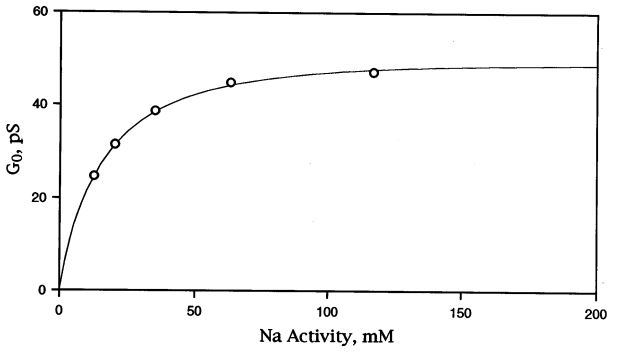

Fig. 7. The same data as in Fig. 3 are fitted with Eqs. (15) and (16), assuming that a surface charge density of 0.002 electronic charges/Å^2 is distributed over the external membrane-solution interface. The K_M of the channel is 30 mM, more than two times larger than the K_M calculated for zero surface charges. It would be impossible to fit the data if a similar charge were distributed on both interfaces.

Culture to Y.K. and to S.O. S.C. was supported by a fellowship from the Japan Society for the Promotion of Science.

References

Ascher, P., Nowak, L. 1988. The role of divalent cations in the N-methyl-D-aspartate responses of mouse central neurones in culture. *J. Physiol.* **399:**247–266

Bliss, T.V.P., Collingridge, G.L. 1993. A synaptic model of memory: long-term potentiation in the hippocampus. *Nature* **361:**31–39

Butler, J.N. 1968. The thermodynamic activity of calcium ion in sodium chloride-calcium chloride electrolytes. *Biophys. J.* **8:**1426–1433

Chang, H., Ciani, S., Kidokoro, Y. 1994. Ion permeation properties of the glutamate receptor channel in cultured embryonic *Drosophila* myotubes. *J. Physiol.* **476:**1–16

Cull-Candy, S.G., Usowicz, M.M. 1987. Multiple-conductance channels activated by excitatory amino acids in cerebellar neurons. *Nature* **325:**525–528

Hamill, O.P., Marty, A., Neher, E., Sakmann, B., Sigworth, F. 1981. Improved patch-clamp techniques for high-resolution current recording from cells and cell-free membrane patches. *Pfluegers Arch.* **391:**85–100

Hille, B. 1984. Ionic channels of excitable membranes. Sinauer Associates, Sunderland, MA

Iino, M., Ozawa, S., Tsuzuki, K. 1990. Permeation of calcium through excitatory amino acid receptor channels in cultured rat hippocampal neurones. *J. Physiol.* **424:**151–165

Jahr, C.E., Stevens, C.F. 1987. Glutamate activates multiple single channel conductances in hippocampal neurons. *Nature* **325:**522–525

Jahr, C.E., Stevens, C.F. 1993. Calcium permeability of the N-methyl-D-aspartate receptor channel in hippocampal neurons in culture. *Proc. Natl. Acad. Sci. USA* **90:**11573–11577

Johnson J.W., Ascher, P. 1990. Voltage-dependent block by intracellular Mg^{2+} on NMDA-activated channels. *Biophys. J.* **57:**1085–1090

Kutsuwada, T., Kashiwabuchi, N., Mori, H., Sakimura, K., Kushiya, E., Araki, K., Meguro, H., Masaki, H., Kumanishi, T., Arakawa, M., Mishina, M. 1992. Molecular diversity of the NMDA receptor channel. *Nature* **358:**36–41

Läuger, P. 1973. Ion transport through pores: a rate theory analysis. *Biochem. Biophys. Acta* **311:**423–441

Mayer, M., Westbrook, G.L. 1987. Permeation and block of N-methyl-D-aspartic acid receptor channels by divalent cations in mouse cultured central neurones. *J. Physiol.* **394:**501–527

McLaughlin, S. 1989. The electrostatic properties of membranes. *Annu. Rev. Biophys. Biophys. Chem.* **18:**113–136

McLaughlin, S.G.A., Szabo, G., Eisenman, G. 1971. Divalent ions and surface potential of charged phospholipid membranes. *J. Gen. Physiol.* **58:**667–687

Methfessel, C., Witzemann, V., Takahashi, T., Mishina, M., Numa, S., Sakmann, B. 1986. Patch clamp measurements on *Xenopus laevis* oocytes: currents through endogenous channels and implanted acetylcholine receptor and sodium channels. *Pfluegers Arch.* **407:**577–588

Nowak, L., Bregestovski, P., Ascher, P., Herbet, A., Prochiantz, A. 1984. Magnesium gates glutamate-activated channels in mouse central neurones. *Nature* **307:**462–465

Premkumar, L.S., Auerbach, A. 1996. Identification of a high affinity divalent cation binding site near the entrance of the NMDA receptor channel. *Neuron* **16:**869–880

Press, W.H., Flannery, B.P., Teukolsky, S.A., Verrerling, W.T. 1988. Numerical Recipes in C. Cambridge University Press, Cambridge, New York

Robinson, R.A., Stokes, R.H. 1959. Electrolyte Solutions, 2nd Ed., revised. Butterworths, London

Rothman, S.M., Olney, J.W. 1987. Excitotoxicity and the NMDA receptor. *Trend. Neurosci.* **10:**299–302

Ruppersberg, J.P., Kitzing, E.V., Schoepfer, R. 1996. The mechanism of magnesium block of NMDA receptors. *Neurosci.* **6:**87–96

Shatkay, A. 1968. Individual activity of calcium ions in pure solutions of $CaCl_2$ and in mixtures. *Biophys. J.* **8:**912–919

Spangler, S.S. 1972. Expansion of the constant field equation to include both divalent and monovalent ions. *Alabama J. Med. Sci.* **9:**218–223

Stern, P., Behe, P., Schoepfer, R., Colquhoun, D. 1992. Single-channel conductances of NMDA receptors expressed from cloned cDNAs: comparison with native receptors. *Proc. Roy. Soc. Lond.* **250:**271–277

Tsuzuki, K., Mochizuki, S., Iino, M., Mori, H., Mishina, M., Ozawa, S. 1994. Ion permeation properties of the cloned mouse ϵ_2/ζ_1 NMDA receptor channel. *Mol. Brain Res.* **26:**37–46

Zarei, M.M., Dani, J.A. 1994. Ionic permeability characteristics of the N-methyl-D-aspartate receptor channel. *J. Gen. Physiol.* **103:**231–248

Appendix

Derivation of the Equation for the Current According to a ''Three-barrier, Two-site'' Model

Figure 8*B* shows that a ''one-ion, three-barrier'' channel has three states of occupancy with one permeant ion species, and five with two. According to the Eyring-Läuger theory, the rate constants for ion movement are exponential functions of the voltage. For example, if one assumes (as we do) that the peaks of the barriers are halfway between neighboring sites, the rate constant for crossing the central barrier from left to right (outward current), λ', is given by

$$\lambda' = \overline{\lambda}' \exp(z\beta^{\phi}/_2) \text{ with } \phi = \frac{FV}{RT} \tag{A1}$$

where z is the valency, V is the voltage across the channel, $\beta/2$ is the electrical distance between the site and the peak of the barrier, and a bar is used to denote the voltage-independent component of the rate constants. The indices $'$ and $''$, when applied to the rate constants, denote outward and inward directions, respectively (*see* also Fig. 8*A*). The voltage-independent factor of the rate constants (e.g., $\overline{\lambda'}$ in Eq. (A1)), is related to the free energy of activation per unit mole, ΔG, and to the temperature, T, by the equation:

$$\overline{\lambda'} = ({}^{kT}/_{h})\exp({}^{\Delta G}/_{RT}) \tag{A2}$$

k, h and R being the Boltzmann, the Planck and the gas constants, respectively. Note that the two rates for entering the channel, ν' and ν'' are proportional to the ion activities, so that we will have:

$$\nu' = \rho' a', \ \nu'' = \rho'' a'' \tag{A3}$$

implying that the dimensions of the two quantities, ρ' and ρ'', ($s^{-1}\,M^{-1}$), are different from those of the rate constants, λ and μ, (s^{-1}). Due to ''microscopic reversibility,'' we shall have:

$$\overline{\rho'}\,\overline{\lambda'}\,\overline{\mu'} = \overline{\rho''}\,\overline{\lambda''}\,\overline{\mu''} \tag{A4}$$

Using well known methods (e.g., *see* Chang et al., 1994), the current-voltage relation for the case of only one permeant ion (e.g., Na^+) is given by:

$$i = \frac{|e|\,\overline{\rho'_{Na}}\,\overline{\lambda'_{Na}}\{a'_{Na}\exp({}^{\phi}/_{2}) - a''_{Na}\exp({}^{-\phi}/_{2})\}}{\overline{\mu''_{Na}}[Q_{Na}(\phi) + a'_{Na}R_{Na}(\phi) + a''_{Na}S_{Na}(\phi)]} \tag{A5}$$

where $a'_{Na}$and a''_{Na} are the activities of internal and external Na^+, respectively. $|e|$ is the absolute value of the electron charge. $\overline{\rho'_{Na}}$, $\overline{\lambda'_{Na}}$, and $\overline{\mu''_{Na}}$ are the voltage-independent factors of rate constants defined in Fig. 8A, and the three functions of the voltage, $Q_{Na}(\phi)$. $P_{Na}(\phi)$ and $S_{Na}(\phi)$, in the denominator, are:

$$Q_{Na}(\phi) = \exp\{z_{Na}(\gamma-\alpha)^{\phi}/_{2}\} + \frac{\overline{\lambda''_{Na}}}{\overline{\mu'_{Na}}}\exp\left\{-z_{Na}(\alpha+\beta)\frac{\phi}{2}\right\} + \frac{\overline{\lambda'_{Na}}}{\overline{\mu''_{Na}}}\exp\left\{z_{Na}(\beta+\gamma)\frac{\phi}{2}\right\} \tag{A6}$$

$$R_{Na}(\phi) = \frac{\overline{\rho'_{Na}}}{\overline{\mu''_{Na}}}\left[\exp\{z_{Na}(\alpha+\gamma)^{\phi}/_{2}\} + \frac{\overline{\lambda''_{Na}}}{\overline{\mu'_{Na}}}\exp\{z_{Na}(\alpha-\beta)^{\phi}/_{2}\} + \frac{\overline{\lambda'_{Na}}}{\overline{\mu'_{Na}}}\exp\{z_{Na}(\alpha+\beta)^{\phi}/_{2}\}\right] \tag{A7}$$

$$S_{Na}(\phi) = \frac{\overline{\rho'_{Na}}}{\overline{\mu''_{Na}}}\left[\exp\{z_{Na}(\alpha+\gamma)^{\phi}/_{2}\} + \frac{\overline{\lambda'_{Na}}}{\overline{\mu'_{Na}}}\exp\{z_{Na}(\beta-\gamma)^{\phi}/_{2}\} + \frac{\overline{\lambda''_{Na}}}{\overline{\mu''_{Na}}}\exp\{z_{Na}(\beta+\gamma)^{\phi}/_{2}\}\right] \tag{A8}$$

The meaning of all the rate constants $\overline{\rho},\overline{\gamma},\overline{\mu}$ as well as that of the electrical distances α,β,γ, should be clear from inspection of Fig. 8*A*. If we now denote the numerator and the denominator of Eq. (A5) by N_{Na} and D_{Na}, respectively, the equation for the current in the presence of solutions containing Na^+-Ca^{2+} mixtures, with Ca^{2+} in the external solution only, is given by:

$$i = \frac{N_{Na} - 2\left(\dfrac{Q_{Na}}{Q_{Ca}}\right)(|e|\overline{\lambda''}_{Ca}\overline{\rho''}_{Ca}/\overline{\mu'}_{Ca})a''_{Ca}e^{-\phi}}{D_{Na} + \left(\dfrac{Q_{Na}}{Q_{Ca}}\right)a''_{Ca}S_{Ca}} \tag{A9}$$

a''_{Ca} is the activity of Ca^{2+} in the external solution, $\overline{\lambda''}_{Ca},\overline{\rho''}_{Ca},\overline{\mu'}_{Ca}$ are rate constants for Ca^{2+}, while Q_{Ca} and S_{Ca} (where the specification, (ϕ), that they are voltage-dependent, has been omitted to shorten the equation) are similar to the quantities in Eqs. (*A6*) and (*A8*), provided that the subscript Na is replaced by Ca, and that z_{Na} is replaced by z_{Ca}. Equation (A9) was used to fit the data in ion mixtures.

Derivation of Equation (11) and (12) from the Goldman-Hodgkin-Katz Equation for the Current

The G-H-K equation for the flux of an ion with valency z is:

$$J = zP\phi\,\frac{a'\exp(z\phi) - a''}{\exp(z\phi) - 1} \tag{A10}$$

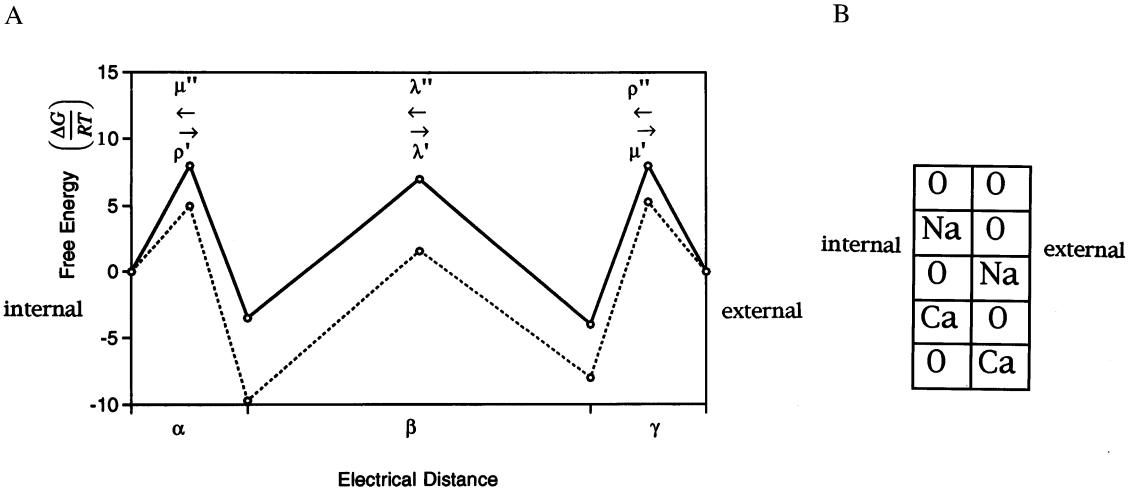

Fig. 8. Diagram of the three-barrier model. (*A*) a three-barrier, two-site model. The heights of the barriers and the depths of the sites (both for Na^+, solid line and for Ca^{2+}, dotted line) were estimated from the fitting values of the rate constants, using Eq. (A2). The free energies in the ordinate are in units of RT (T = 300° K) (*B*) states of occupancy of the channel in the presence of two permeant ions.

where ϕ is the membrane potential normalized in units of *RT/F*. In a mixture of Na^+ and Ca^{2+}, the membrane current per unit area will be:

$$I = F(J_{Na} + 2\,J_{Ca}) \tag{A11}$$

Substitution of J_{Na} and J_{Ca} with their expressions given by equation (A10) yields an explicit equation for the current per unit area. Equation (11) of the text can be easily arrived at by imposing the condition of zero current, approximating the concentrations of internal calcium with zero ($C'_{Ca} = 0$), and taking note of the fact that $[\exp(2\phi) - 1]$ (which appears in the denominator of J_{Ca}) is equal to $[\exp(\phi) - 1]\,[\exp(\phi) + 1]$. Finally, Eq. (12) is obtained by recognizing that Eq. (11) is a quadratic equation in $\exp(\phi)$, and solving it with the usual elementary methods.

Derivation of Equation (15), the Channel ''Zero-Current Conductance,'' for a Membrane Bearing a Negative Surface Charge Density on the Interface with the External Solution

For simplicity we shall now consider a ''one-site, two-barrier'' model for a channel, assuming: (i) that a negative surface charge density is present only on the external interface, (ii) that the solutions are symmetrical and (iii) that they contain only one monovalent electrolyte, the cation in the electrolyte being the sole permeant species through the channel. Conditions (ii) and (iii) were satisfied in the experimental conditions corresponding to Figs. 1 and 2. Since a negative surface potential will be present at the interface with the external solution ($x = d$), the cation concentrations at the two interfaces, $C(0)$ and $C(d)$, will be

$$C(0) = C \text{ and } C(d) = C\exp(-\phi_S) \tag{A12}$$

where C is the concentration of the electrolyte (and thus also of the permeant cation) in the bulk solutions, and ϕ_S, is the surface potential, normalized in units of *RT/F*. The normalized potential difference between the two bulk solutions (inside-outside) will be:

$$\phi_T = \phi + \phi_S \tag{A13}$$

where the first term on the right hand side, ϕ, is the transmembrane potential difference between the two membrane-solution interfaces. One can now follow a procedure completely analogous to that used to derive equation (A5), recalling however that in a ''two-barrier'' model there are only four rate constants: $\overline{\rho'}$,$\overline{\mu'}$,$\overline{\rho''}$,$\overline{\mu''}$, related by microscopic reversibility, $\overline{\rho'}\,\overline{\mu'} = \overline{\rho''}\,\overline{\mu''}$, and only two electrical distances, α,β, with the obvious condition that $\alpha + \beta = 1$. The equation for the current is found to be:

$$i = \frac{\overline{\rho''}\,|e|\,[C(0)\exp(\phi/2) - C(d)\exp(-\phi/2)]}{Q^*_{Na} + R^*_{Na} + S^*_{Na}} \tag{A14}$$

where

$$Q^*_{Na} = exp(-\alpha\phi/2) + \frac{\overline{\mu'}}{\overline{\mu''}}\exp(\beta\phi/2)$$

$$R^*_{Na} = \frac{C(0)}{K_M}\exp(\alpha\phi/2) \tag{A15}$$

$$S^*_{Na} = \frac{C(d)}{K_M}\frac{\overline{\mu'}}{\overline{\mu''}}\exp(-\beta\phi/2)$$

K_M being defined as $\overline{\mu''}/\overline{\rho'}$, or (due to microscopic reversibility) $\overline{\mu'}/\overline{\rho''}$. Equation (15) of the text can now be obtained by substituting Eqs. (A12) and (A13) in Eqs. (A14) and (A15), dividing by the total membrane potential, V_T (which is related to the normalized potential, ϕ_T, by $VT = RT\phi_T/F$), and finally taking the limit for $V_T \to 0$.

To obtain Eq. (18), one must only note that at low C Eq. (16) is approximated by $e^{-\phi_S} \cong A/C$, that the only surviving term in the denominator of Eq. (15) at low C is the second, and that, because of microscopic reversibility, $\overline{\rho''}\,\overline{\mu''}/\overline{\mu'} = \overline{\rho'}$.

Note Added in Proof

In a recent and very interesting study of the same channel expressed in *Xenopus* oocytes, Premkumar and Auerbach (1996) found single-channel conductances (86 pS) in the presence of 100 mM Na^+ on both sides that are much higher than those reported in this paper (50 pS with 153.8 mM Na^+). While the discrepancy may be partly due to the fact the authors used external EGTA to buffer Ca^{2+}, their titration curves indicate that the conductance remains high even for Ca^{2+} concentrations equal to 5×10^{-7} or 10^{-8} M, values that are similar to those present in our experiments with 'nominally' pure Na^+ (about 0.55 μM Ca^{2+}, Figs. 1, 2 and 3). Thus, the full reason for the discrepancy is not well understood, although it seems appropriate to emphasize that the conductance values found in our study are in agreement with several ones reported previously in the literature on the same channels under similar conditions in the absence of external Ca^{2+} (55.5 pS in cultured mouse neurons, Ascher & Nowak, 1988; 65.6 pS, in cultured rat neurons, Jahr & Stevens, 1993; 70 pS in *Xenopus* oocytes, Ruppersberg et al., 1994).

Moreover, although Premkumar and Auerbach (1996) do not show a curve for the conductance as a function of Na^+ concentration in symmetrical solutions, they report a value for K_m (same as our K_M) which is nine times higher than ours (129 mM instead of 14.7 mM), and ten times higher than that found by Zarei and Dani (1994) for NH_4^+ (12 mM). Since the authors of the last quoted study used EGTA and EDTA in the external solutions, it is not clear whether the use of the divalent chelator is the sole cause for these discrepancies.